DOI: 10.1002/chem.200801469

# Sonochemical Synthesis under a Magnetic Field: Fabrication of Nickel and Cobalt Particles and Variation of Their Physical Properties

**Riam Abu-Much* and A. Gedanken*[a]**

**Abstract:** We report on the variation of the physical properties of nickel and cobalt nanoparticles prepared by using ultrasound irradiation as energy source. First, we describe a sonochemical method for preparing aggregated particles. Second, we interpret the results on the basis of Einstein's theory (1905), which deals with a mathematical expression for the diffusivity of particles into solvents. This theory explains the stability of organosols of nickel and cobalt nanoparticles in polyethylene glycol. Finally, the effect of applying an external magnetic field during sonochemical formation of both aggregated particles and their stable colloids is investigated.

**Keywords:** cobalt · colloids · nanostructures · nickel · sonochemistry

## Introduction

A fundamental of the physics and chemistry of solids is the understanding that most of their properties depend significantly on the size of a solid particle in one, two, or three dimensions. Whether it can be called a revolution or simply continuous evolution, the development of new materials and their understanding on an increasingly smaller length scale is clearly at the root of progress in many areas of materials science.[1] This is particularly true in the development of new magnetic materials for a variety of important applications.[2–5] Nanoscale magnetic materials have attracted intensive interest because of their potential applications in fields such as high-density magnetic recording and magnetic sensors. In addition, the nanoscale magnetic materials also enabled some basic issues of magnetic phenomena in low-dimensional systems to be addressed.[6–9] Ferromagnetic metallic materials such as Fe,[10,11] Co,[12–14] and Ni[15,16] have been studied for many years. During the last decade, due to the emergence of a new generation of high-technology materials, the number of groups involved in nanomaterials research has increased exponentially. Various approaches have been developed to prepare nanoscale magnetic metal materials, including pyrolysis of metal carbonyls,[17,18] water-in-oil microemulsions,[19] γ-ray irradiation,[20] borohydride reduction of metal salts,[21] and template synthesis.[22] The study of colloidal magnetic fluids is of increasing interest in different technological areas, from mechanical antivibration systems to biomedical applications.[23–25] These fluids are suspensions of ferri- or ferromagnetic particles dispersed in aqueous or nonaqueous carrier liquids. Since their initial synthesis in the 1960s, their technological applications have continued to expand.[26] Different kinds of ferrofluids (FFs), such as water-based FFs and FFs based on organic compounds, have been obtained and widely used in dynamic loudspeakers, computer hardware, dynamic sealing,[29] electronic packing, mechanical engineering, aerospace applications, and bioengineering.[30] Particle content, saturation magnetization, suspension viscosity, and surfactant stabilizers[31] are vital for product performance.[32] The stability of ferrofluids depends on a balance between repulsive and attractive interactions among the magnetic nanoparticles.[27] In addition to thermal motion, steric and electrostatic repulsive interactions act against van der Waals and dipolar attractive interactions.[28] For a stable FF, the repulsion should be at least as strong as the attractive forces in the range of the attractive interaction. Stability can be obtained by surrounding the colloidal particles with an electrical double layer, adsorbed or chemically attached polymeric molecules, or with free polymers in the dispersion medium (depletion/stabilization).

The depletion/stabilization of colloidal particles is imparted by macromolecules that are free in solution, and their free polymer chains can play a crucial role in preventing aggregation of the particles. A variety of innovative techniques

[a] Dr. R. Abu-Much, Prof. A. Gedanken
Department of Chemistry and Kanpar Laboratory for Nanomaterials
Bar-Ilan University Center for Advanced Materials
and Nanotechnology
Bar-Ilan University, Ramat-Gan 52900 (Israel)
Fax: (+97) 235-351-250
E-mail: riamab@gmail.com
gedanken@mail.biu.ac.il

   

have been employed to prepare cobalt and nickel nanomaterials, for example, template electrodeposition[33] and rapid decomposition in the presence of linear amines.[34] In general, chemical dissolution techniques are superior to the other methods because of their better capabilities for controlling the composition, size, and shape of the nanoparticles, and the ease of scale-up. This is especially true for the precipitation of metals from aqueous solutions of metal salts with hydrazine or hydrogen as reducing agents.[35] The polyol process, in which a polyol or a mixture of polyols is used as both solvent and reducing agent, can be used to prepare more uniform and well-dispersed metal powders (e.g., Ni, Co) in comparison with other chemical reduction methods, because the polyol process is slow and requires high temperatures and refluxing for several hour, or even days.[36,37] This reflux helps to form a more uniform distribution of nanoparticles through cycles of dissolution/precipitation, as in the previously described process of Ostwald ripening.

Little attention has been paid to the effect of an external magnetic field on the nucleation and growth process of magnetic particles, and on the self-assembly behavior of magnetic nanocrystallites. A magnetic field can significantly influence the movement of magnetic particles.[38–40] It is therefore interesting to study the growth behavior of magnetic particles during their fabrication under an external magnetic field. Recent developments have indicated that a magnetic field can be elegantly employed to orient self-assembling magnetic nanoparticles into nano- or microscale structures in which dipole interactions between adjacent magnetic nanoparticles couple them together and force reversible formation of an anisotropic structure.[40–44] These magnetic nanoparticles encompass fascinating aspects such as superparamagnetism, dipolar interactions, and Zeeman energy. One- to three-dimensional (1D to 3D) self-assembled structures of magnetic nanoparticles have been synthesized through magnetic interactions and the application of a magnetic field.[45–51]

In the current work we first explored the feasibility of sonochemical fabrication of nickel and cobalt particles, variation of their size, and formation of colloidal solutions with different solvents. Second, we studied the effect of applying a magnetic field during fabrication.

Ultrasound influences chemical reactivity through an effect known as cavitation. Cavitation occurs on applying high-intensity ultrasound to liquids, which results in superposition of sinusoidal pressure on the steady ambient pressure. Sound is transmitted through a fluid as a wave consisting of alternating compression and rarefaction cycles. In cavitation, the microbubbles formed during the rarefaction cycle of the acoustic wave collapse violently during the compression cycle of the wave. The contents of the bubble are estimated to be heated to 5000 K, and the implosion of the cavitation bubble also produces high-energy shock waves with pressures of several thousand atmospheres.[52] The ultimate consequence of the high temperature is a chemical reaction. The high pressure leads to an increased number of molecular collisions owing to enhanced molecular mobility and decreased overall volume, and hence also to high chemical reactivity.

## Results and Discussion

**Characterization of Ni and Co particles**: Sonochemical reactions involve a combination of high temperatures, high pressures, and rapid cooling. Under these extreme conditions, fine cobalt and nickel spheres are produced.

The X-ray diffraction pattern of an as-prepared Ni sample (Figure 1a) confirms the crystalline nature of the particles.

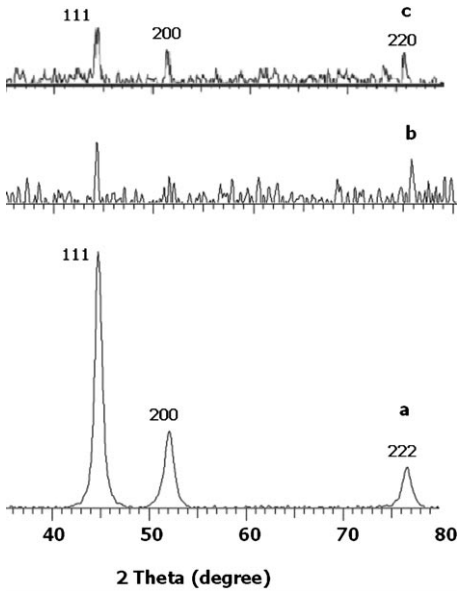


Figure 1. a) XRD pattern of as-prepared nickel particles. b) XRD pattern of as-prepared cobalt particles. c) XRD pattern of cobalt particles after heating to 600 °C

The three characteristic peaks that appear at $2\theta$ values of 44.7, 52.07, and 76.63° are assigned to diffractions from the (111), (200), and (222) planes of cubic Ni. The calculated cell parameter is $a = 3.514$ Å. These values are in good agreement with the diffraction peaks, peak intensities, and cell parameters of cubic Ni (PDF No. 00-003-1051). The XRD patterns of the as-prepared cobalt spheres and the product after annealing at 600 °C for 6 h, are presented in Figure 1b and c, respectively. The as-prepared sample shows low-intensity diffraction peaks indicating production of poorly crystalline cobalt, whereas the heated sample shows sharp diffraction peaks that could be indexed to fcc cobalt (PDF No. 00-0001-1255). The morphology and structure of the aggregated particles obtained both by the regular sonication procedure and sonication under a magnetic field were studied by HRSEM and HRTEM measurements. HRSEM images with different magnifications are presented in Figure 2. Figure 2a and d show nanospheres of Ni and cobalt formed in the absence of a magnetic field. Characterization of the spheres as pure nickel or pure cobalt was

  

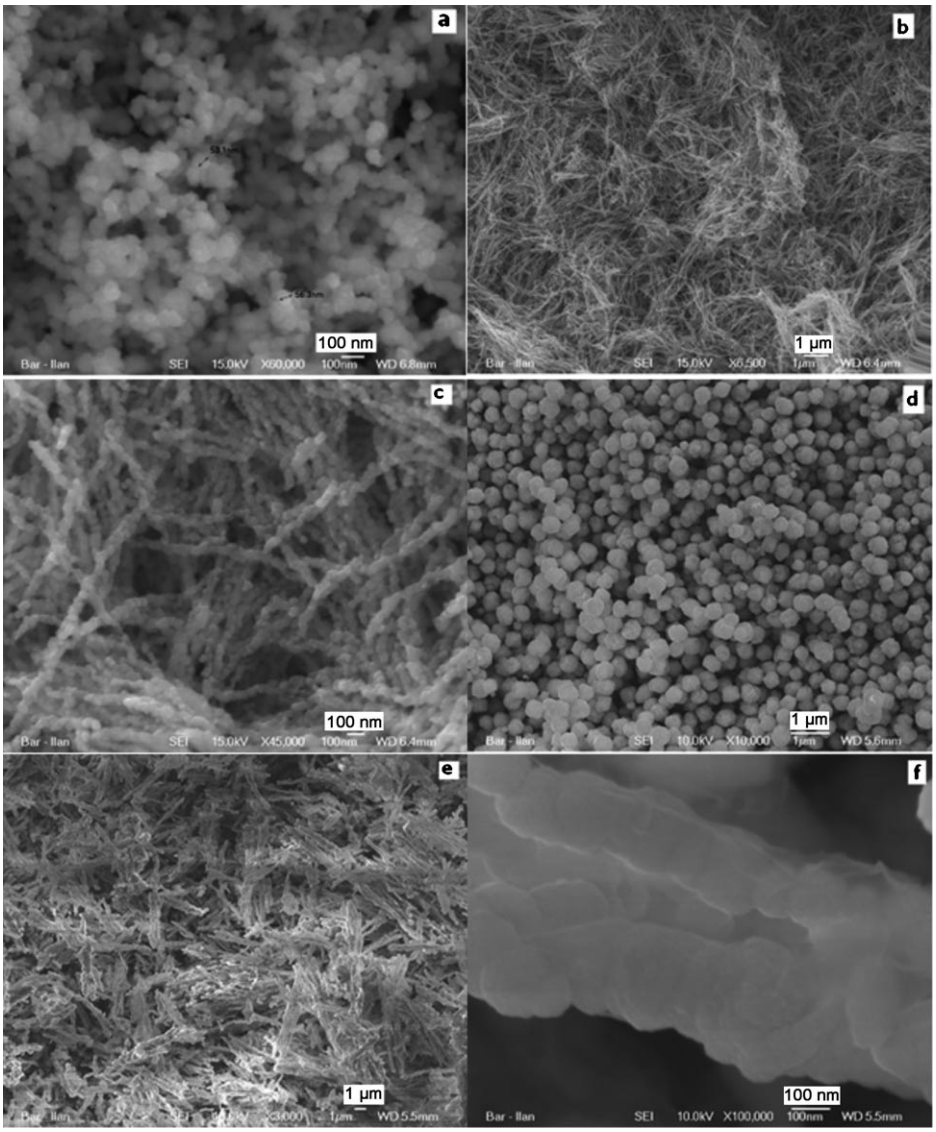


Figure 2. SEM images of nickel and cobalt particles. a) Nickel particles synthesized by the regular sonication procedure. b, c) Nickel nanowires prepared in the presence of an applied magnetic field. d) Cobalt particles prepared by the regular sonication process. e, f) Cobalt nanowires synthesized under a magnetic field.

based not only on XRD but also on selected-area electron diffraction (SAED) analysis conducted on the SEM images (not shown). In both cases, this showed the presence of a high percentage of Ni or Co and the C and Cu peaks originating from the carbon grid. The average diameter of the nickel spheres, calculated by using Scion Image software, was 52 nm, whereas bigger spheres are obtained for cobalt particles. Their average size, calculated from an SEM image, was 350 nm. Conducting the sonication process under an external magnetic field has a significant influence on the morphology of both cobalt and nickel particles. On the basis of these results, it can be concluded that the major factor determining the size and morphology of the products is the magnetic field. Figure 2b, c, e, and f vividly demonstrate the creation of nanowires. The high-magnification images show that the nanowires are produced as a consequence of the aggregation mechanism of the magnetic spheres driven by strong magnetostatic (dipolar) and Zeeman interactions. HRTEM analysis provided more detailed structural information on Ni and cobalt particles obtained both by the regular sonication procedure and under an external magnetic field. Figure 3a further supports the crystalline nature of nickel particles obtained sonochemically. In the absence of a magnetic field, the interlayer distance was calculated to be about 2.01 Å, which agrees well with the literature value for the separation between the (111) lattice planes. Similar results were obtained for Ni rods prepared under a magnetic field. For the cobalt particles it was more difficult to recognize the arrangement of atomic layers because of their low crystallinity. Nevertheless, the measured distance of about 2.1 Å between the (111) lattice planes (Figure 3b) is very close to that reported in the literature for the fcc crystal structure.

The differences between the nickel and cobalt particles obtained without and with an external magnetic field were also reflected in differences in the magnetic properties. Figure 4 shows magnetization loops of the products. They reveal that the magnetic structure of Ni and Co particles can be modified during their formation under a magnetic field. Differen-

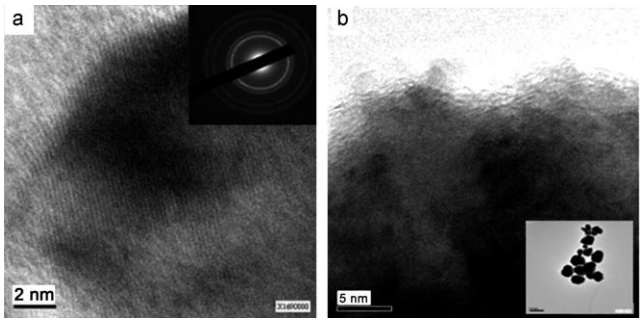


Figure 3. a) HRTEM image of a nickel particle. b) HRTEM image of a cobalt particle.

  

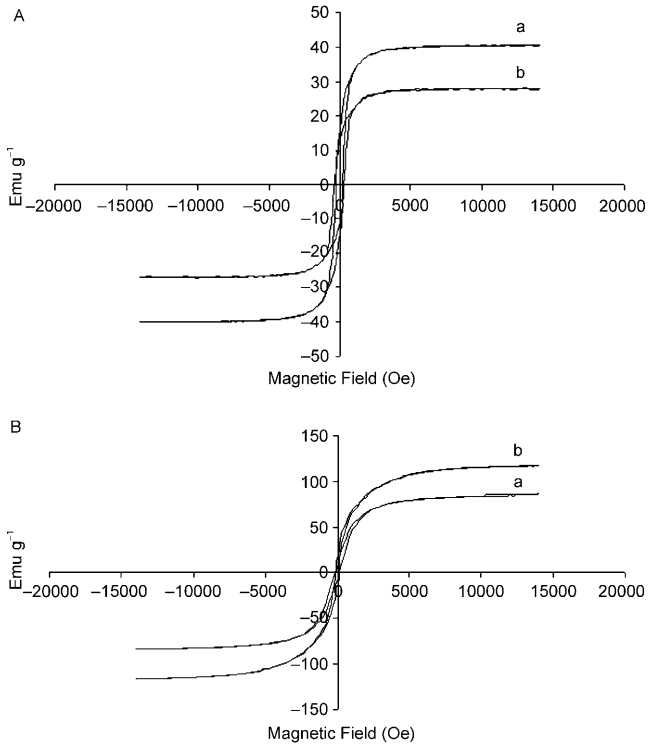


Figure 4. A) Magnetization loop of nickel particles obtained without a magnetic field (a) and magnetization loop of nickel particles obtained under a magnetic field (b). B) Magnetization loop of cobalt particles obtained without a magnetic field (a) and magnetization loop of cobalt particles obtained under a magnetic field (b).

ces in saturation magnetization $M_s$ between samples obtained under an external magnetic field and those obtained without an applied magnetic field are clearly evident. The difference in $M_s$ between the samples prepared with and without a magnetic field can be attributed to spin disorder and surface oxidation. The magnetic behavior of nanoparticles has a marked dependence on the decrease in particle size and when surface effects start to dominate.[42] For nanoparticles with a large surface/volume ratio, the surface-spin-driven arrangements (spin disorder) may eventually modify the magnetic properties. This spin disorder is caused by the lower coordination number of the surface atoms, whereby broken exchange bonds produce a spin-glass-like state of spatially disordered spins on the surface with a high-anisotropy surface layer.[43,44] In addition, the change in the magnetic structure can be also the reason why, when a magnetic field is applied, the magnetic easy axis of nickel could align along the nanowires. This may be also responsible for the increase in the saturation magnetization of the cobalt particles, as can be seen in Figure 4B. However, the reason for the low saturation magnetization of the nickel particles obtained under an MF (Figure 4A) is not clear. Perhaps the large shape anisotropy of the nanorods prevents their becoming magnetized in directions other than their easy magnetic axis. Our assumption is related to a random orientation of nanorods, for which the projection of the magnetization vectors along the field direction is smaller than that of a collection of nanoparticles without the large shape-anisotropy effect.

We also measured the magnetic moment as a function of temperature for nickel particle prepared by the regular sonication process and under an external magnetic field by three procedures: 1) The samples were zero-field-cooled (ZFC) to 5 K, a field was applied, and the magnetization was measured as a function of temperature; 2) The samples were field-cooled (FC) from above 300 to 5 K and the magnetization was measured; 3) The samples were field-cooled to 5 K, after which the field was reversed in sign and the magnetization was measured as a function of temperature (RFC). The results are shown in Figure 5.

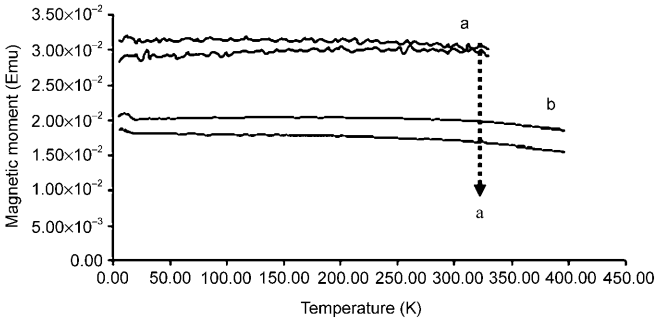


Figure 5. Magnetic moment versus temperature. a) Nickel particles prepared without applied magnetic field. b) Nickel particles prepared under a magnetic field.

Below the blocking temperature $T_B$, the ZFC and FC curves do not coincide. Above $T_B$ they coincide, and the materials exhibit superparamagnetic behavior. The blocking temperature of the samples obtained without a magnetic field ($T_B \approx 320$ K) is lower than that of the sample synthesized in the presence of a magnetic field ($T_B \gtrsim 400$ K). This difference is accounted for by the relation $T_B = KV/25k$, where $K$ is the effective uniaxial anisotropy energy per unit volume, $V$ is the particle volume, and $k$ the Boltzmann constant. The $K$ and $V$[54] values of the rods obtained with applied magnetic field are larger than those of the products obtained without a magnetic field. The blocking temperature of these rods is therefore higher. The blocking temperature also depends on size, shape, and material, and it usually increases with increasing number of atoms. Shape also matters: Nanorods usually have a higher blocking temperature than nanodots.

**Significant decrease in particle size and formation of stable organosols in PEG-400**: We sought a facile and direct method for fabrication of stable organosols of nickel and cobalt nanoparticles. The main aim was to significantly decrease the particle size and hence obtain a stable dispersion. This was achieved by restricting the growth process and limiting the collision rate between particles. This was effected by varying the physical properties of the solvent.

Using triethylene glycol as solvent instead of ethylene glycol gave smaller particles of both nickel and cobalt, but a

  

stable colloidal solution was not obtained. Unlike the corresponding reaction in ethylene glycol, in which a precipitate was observed immediately after sonication, in triethylene glycol it took about 30 min for the precipitate to appear. According to the HRSEM images (Figure 6), nickel and cobalt

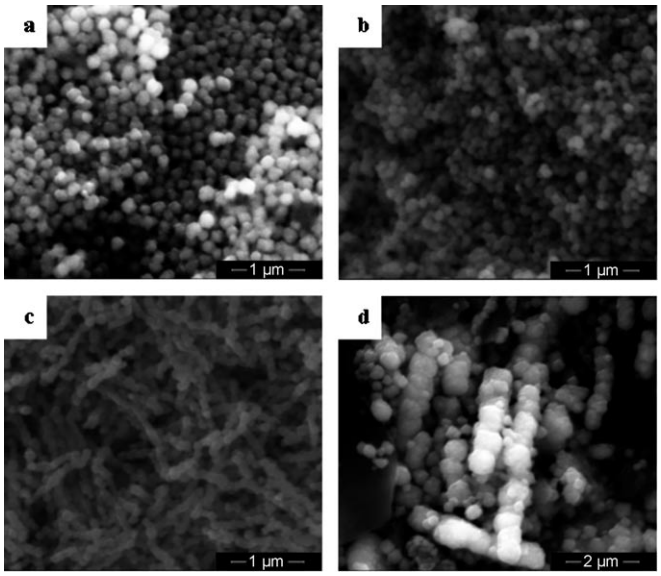


Figure 6. HRSEM images of nickel and cobalt particles. Nickel (a) and cobalt (b) particles synthesized by the regular sonication procedure in triethylene glycol. Nickel (c) and cobalt (d) particles prepared in the presence of an applied MF with ethylene glycol as solvent.

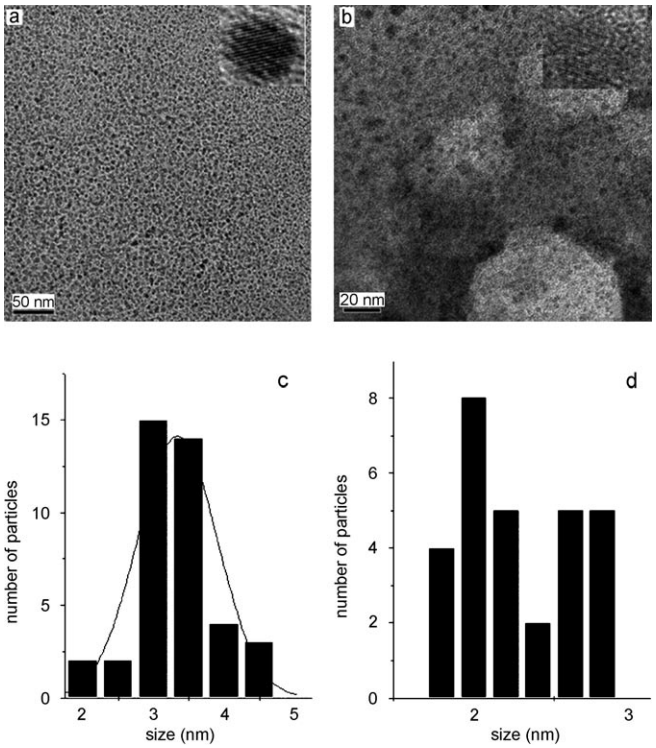


Figure 7. a) HRTEM image of stable organosol of nickel nanoparticles synthesized by the regular sonication procedure. b) HRTEM image of stable organosol of cobalt nanoparticles synthesized by the regular sonication process. c) Histogram of the average size of the nickel nanoparticles from image a). d) Histogram of the average size of the cobalt nanoparticles from image b).

spheres with average particle sizes of 120 and 100 nm, respectively, are produced in triethylene glycol. Compared with the reaction in ethylene glycol, the size of the cobalt spheres has decreased significantly, from 350 to 100 nm. Exposing the reaction cell to an external magnetic field induced assembly of the nanomagnetic particles into macroscopic arrays (Figure 6c, d).

A dramatic effect was observed when polyethylene glycol 400 (PEG-400) was used as solvent in the sonication cell: the higher viscosity and long polymer chains act as physical barriers to aggregation of the particles, which is reflected by the formation of a stable colloidal solution of smaller nanoparticles. The restricted motion of the particles due to the high viscosity and the polymer chains resulted in a slow growth process of the particles, reflected by formation of nanoparticles with average sizes of 3.2 and 2.3 nm for Ni and Co, respectively. Thus, a significant decrease in particle size is obtained by using PEG-400 as solvent instead of ethylene glycol or triethylene glycol. A very stable colloidal solution is obtained for both metals and flocculation, and hence gravitational settling, is avoided. The solutions were stable for at least four months. Figure 7a and b show HRTEM images of the uniform and monodisperse nickel and cobalt nanoparticles with perfect arrangements of the atomic layers. The measured distance between the (111) lattice planes of the Ni nanoparticles of about 2.02 Å is very close to that reported in the literature for cubic nickel (PDF No. 00-003-1051). In addition, the calculated distance between the (111) lattice planes of the FCC cobalt of about 2.0 Å is very close to the literature value (PDF No. 00-0001-1255). The SAEDS results (not shown) confirm the presence of high percentages of Ni and Co, respectively. Histograms of size distribution were calculated by using Scion Image software by measuring more than 40 nanoparticles (Figure 7c, d).

We assume that the stability of the nanoparticles against aggregation is due to the presence of the free polymer chains of the solvent (depletion/stabilization), while its viscosity restricts the growth process of the particles. This is reflected by the formation of very small nanoparticles. The absence of a direct interaction between the polymer chains and the nanoparticles is supported by the FTIR spectra of pristine PEG and organosols of nickel and cobalt nanoparticles. The FTIR spectra of Ni and Co organosols showed no shifts or changes in the intensity of the absorption bands relative to pristine PEG (Figure 8), especially the $\nu_{CO}$ band at about 3400 $cm^{-1}$, which would perhaps be susceptible to changes if PEG and a magnetic metal interact. Surprising results emerged when the effect of applying an external MF during sonochemical preparation of the organosols was studied. In both cases, stable solutions of nickel and cobalt nanoparticles were produced. The influence of the magnetic field

  

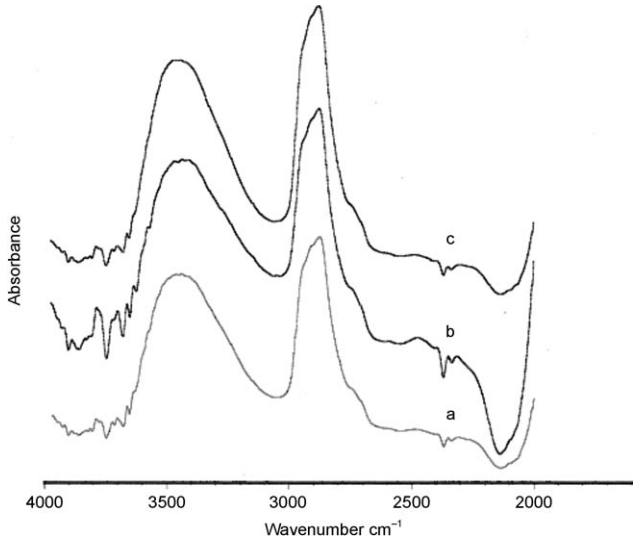


Figure 8. FTIR spectra of a) pristine PEG, b) organosol of nickel nanoparticles in PEG, and c) organosol of cobalt nanoparticles in PEG.

on the morphology of the nanoparticles was investigated by HRTEM analysis, which showed small and uniform nanoparticles (Figure 9). No differences in morphology or size of

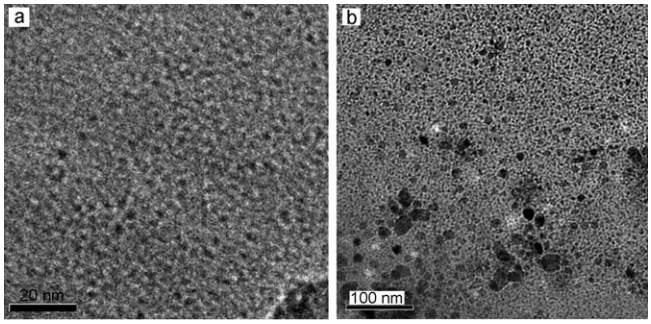


Figure 9. a) HRTEM image of stable organosol of nickel nanoparticles synthesized under a magnetic field. b) HRTEM image of stable organosol of cobalt nanoparticles synthesized under a magnetic field.

the nanoparticles were found. Thus, unlike the Ni and Co reactions under nonstabilized conditions, application of an external magnetic field of 0.5 T during synthesis of these colloidal solutions has no appreciable effect. We argue that, despite the fact that the application of an external magnetic field causes the particles to attain large magnetic moments aligned in the direction of the magnetic field and thus strong magnetic interaction, the restricted motion of the particles due to the high viscosity of the continuous phase and the presence of long polymer chains are the dominant factors. This is also reflected in the formation of small particles, consistent with a slow growth process. These results reveal the importance of the physical properties of the continuous phase. In our case, the interparticle magnetic attraction was too weak to overcome the physical barriers that surround each particle.

## Discussion

In the current investigation, ultrasonic waves served as a source of energy to drive the reactions. The preparation of both nickel and cobalt particles was based on a reduction mechanism using a small amount of hydrazine as a reducing agent.[53] To confirm that the reduction was conducted mainly by hydrazine rather than by ethylene glycol, a control reaction was performed without the addition of hydrazine. No nickel or cobalt was obtained, even after several hours of sonication.

More significant results were obtained by introducing PEG-400 as dispersive medium and stabilizer. It also caused a dramatic decrease in particle size. The presence of polymer chains restricts the growth process and increases the number of nucleation sites. Thus, nanoparticles with average sizes of 3.2 and 2.3 nm for Ni and Co, respectively, were obtained. In contrast, particles with sizes of 52 and 350 nm were formed when ethylene glycol was used as a solvent.

The DLVO theory[55] has traditionally been used to evaluate the onset of aggregation by calculation of stability ratios (i.e., the ratio of the aggregation rate in the absence of colloidal interactions to that when interactions are present). According to this theory, the colloids are the only solute, and electrolytes and solvent effects are captured in an effective interparticle potential. Another significant parameter is the collision efficiency (i.e., the ratio of the number of particle collisions resulting in formation of an aggregate to the total number of collisions). These collisions between the particles are the result of the Brownian motion. The stability of the colloid is thus determined by the interaction between the particles during such a collision. Stability can be obtained by surrounding colloidal particles with an electrical double layer, adsorbed or chemically attached polymer molecules, or a free polymer in the dispersion medium (depletion/stabilization). The depletion/stabilization of colloidal particles is caused by macromolecules that are free in solution. Their free polymer chains can have a crucial role in preventing the aggregation of the particles. According to our results, the stability of the nickel and cobalt sols is due to the presence of free polymer chains. We believe that the viscosity of the PEG solvent plays an important role in the stabilization mechanism. It restricts diffusion of the particles through the dispersion medium, and hence reduces the probability of collision. We based our assumption on the Einstein theory (1905)[56] that deals with a mathematical expression for the diffusivity of colloid particles into solvents. The diffusivity is proportional to $KT/6\pi\mu R_a$, where $\mu$ is the viscosity of the solvent, $K$ the Boltzmann constant, $R_a$ the radius of the colloid spheres, and $T$ the absolute temperature of the solution. According to this equation, increasing the viscosity of the dispersion medium limits the motion of the particles and hence reduces the collision ratio, which could lead to aggregation and sedimentation by gravity.

The extreme conditions that occur when the bubble collapses might lead to the assumption that sonochemistry determines the shape and size of the reaction products, and ap-

  

plication of a magnetic field during sonication would have only a minor effect. This is especially true since the term describing the magnetic dipole interaction does not contain the intensity of the external magnetic field and is proportional only to $\mu_1\mu_2/R^3[2\cos(\theta_1-\theta_2)-3\cos\theta_1\cos\theta_2]$.[54] However, the results obtained with the aggregated nickel and cobalt particles reveal the important role of the magnetic field in determining the shape and magnetic properties of the products. Our explanation of these results is based on the location of the sonochemical reaction. It is well known that the sonochemistry of ionic reactants takes place in the interfacial region of about 200 nm surrounding the collapsing bubble[52] at temperatures and pressures much lower than those developed at the center of the bubble. This diminishes the effect of the ultrasonic event in comparison to a gas-phase reaction which occurs with a volatile precursor. When an external magnetic field is applied during the growth of ferromagnetic particles, particle growth is considered to be a slow diffusion-assisted process. Our investigation revealed that the extreme conditions resulting from sonication can not act as a barrier against the effect of a magnetic field on the growth process of the magnetic nickel and cobalt particles. The magnetic field led to the formation of nanowires rather than sphere-shaped particles when particle aggregation occurred.

A significant result was obtained when we introduced PEG-400 as solvent. Although application of an external magnetic field causes the nanoparticles to attain large magnetic moments aligned in the direction of the magnetic field, and hence a strong magnetic interaction, we found no difference in the morphology and the size of the particles. Moreover, stable colloidal solutions were obtained under these conditions. We argue that the physical parameters responsible for the stabilization mechanism of the nickel and cobalt sols produced by the regular sonication procedure dominate over the magnetic interactions caused by the applied external magnetic field. This is reflected in the stability, morphology, and the size of the particles. Thus, the solvent can affect not only the aggregation process, but also can act as a barrier against external magnetic forces.

## Conclusion

We have synthesized cobalt and nickel particles using ultrasonic irradiation and characterized them. The particle size and morphology depend on the physical properties of the solvent. The influence of an applied magnetic field during sonochemical preparation is also affected by the physical properties of the solution.

## Experimental Section

**General**: Ethylene glycol (J. T. Baker), triethylene glycol (99%, Aldrich), nickel(II) nitrate hexahydrate (Aldrich), hydrazine monohydrate (98%, Aldrich), sodium hydroxide (Bio LAB), polyethylene glycol 400 (Aldrich), and cobalt(II) nitrate hexahydrate (Riedel-de Haen) were used without further purification.

**Synthesis of pure nanometer-sized Ni and Co particles**: Based on the work of Li and Han[53] on the reaction mechanism and kinetics of reduction of metal cations, especially $Ni^{2+}$, by hydrazine, sonochemical syntheses of Ni and Co particles were carried out as follows. Nickel(II) nitrate or cobalt(II) nitrate (0.05 M) was dissolved in ethylene glycol, and hydrazine (2.5 mL, 1 M) was added. The solution was sonochemically irradiated under ambient atmosphere for 30 min with a high-intensity ultrasonic horn (Ti horn, Sonics and Materials VCX600 sonicator, 20 kHz). During sonication, an appropriate amount of NaOH (0.003 M) was added to the solution. The powder obtained was isolated by centrifugation, washed three times with ethanol (9000 rpm), and dried under vacuum at room temperature. The same procedure was carried out by replacing ethylene glycol with triethylene glycol.

**Synthesis of stable organosols of Ni and cobalt nanoparticles**: Nickel(II) nitrate or cobalt(II) nitrate (0.05 M) was dissolved under ultrasound radiation in PEG-400, and hydrazine (2.5 mL) was added. The solution was sonochemically irradiated under ambient atmosphere for 1 h by using a high-intensity ultrasonic horn (Ti horn, Sonics and Materials VCX600 sonicator, 20 kHz). During sonication a desired amount of NaOH (0.003 M) was added gradually. After sonication a black solution was obtained.

**Sonication under an external magnetic field**: The reaction procedures described above were conducted under an external magnetic field of 0.5 T.

**Characterization**: Powder XRD measurements were carried out on a Rigaku model-2028 diffractometer. The morphologies and structures of the as-synthesized products were further characterized with a JEM-1200EX TEM and a JEOL-2010 HRTEM. Samples for TEM and HRTEM were prepared by dispersing the products in ethanol, placing a drop of the suspension onto a copper grid coated with an amorphous carbon film, and then drying under inert atmosphere. HRSEM analyses were conducted with a JEOL-JSM 840 scanning electron microscope. Scion Image software was used to measure the mean particle size by measuring more than 50 particles from the HRSEM images. Magnetization measurements were conducted with a Quantum Design MPMS SQUID magnetometer. First, the blocking temperature was measured by cooling the sample in zero field down to 5 K, at which point a magnetic field of 100 Oe was applied. Then the sample was slowly warmed to high temperature in steps of a few kelvin, with stabilization at each temperature and subsequent measurement of the magnetic moment (zero-field cooled (ZFC) measurement). Then, without turning off the magnetic field, the sample was cooled and the magnetic moment measured at each intermediate temperature (field-cooled (FC) measurements). The stable organosols were further analyzed by IR spectroscopy (Nicolet Impact 410).

[1] H. Gleiter, *Prog. Mater. Sci.* **1989**, *33*, 223.
[2] M. E. McHenry, K. Gallagher, F. Johnson, J. H. Scott, S. A. Majetich in *Recent Advances in Chemistry and Physics of Fullerenes and Related Materials*, ECS Symposium Proceedings, Pennington, NJ, **1996**, p. 703.
[3] M. E. McHenry, S. A. Majetich, M. De Graef, J. O. Artman, S. W. Staley, *Phys. Rev. B* **1994**, *49*, 11358.
[4] M. E. McHenry, S. Subramoney, *Fullerenes: Chemistry Physics and Technology*, in press.
[5] M. E. McHenry, M. A. Willard, H. Iwanabe, R. A. Sutton, Z. Turgut, A. Hsiao, D. E. Laughlin, *Bull. Mater. Sci.* **1999**, *22*, 425.
[6] J. L. Dormann, D. Fiorani, E. Tronc, *Adv. Chem. Phys.* **1998**, 283.
[7] D. L. Leslie-Pelecky, R. D. Rieke, *Chem. Mater.* **1996**, *8*, 1770.
[8] R. H. Kodama, *J. Magn. Magn. Mater.* **1999**, *200*, 359.
[9] V. Skumryev, S. Stoyanov, Y. Zhang, G. Hadjipanayis, D. Givord, J. Nogues, *Nature* **2003**, *423*, 850.
[10] T. Jonsson, P. Svedlindh, M. F. Hansen, *Phys. Rev. Lett.* **1998**, *81*, 3976.
[11] X. X. Zhang, J. M. Hernandez, J. Tejada, R. F. Ziolo, *Phys. Rev. B* **1996**, *54*, 4101.

  

[12] X. X. Zhang, G. H. Wen, G. Xiao, S. H. Sun, *J. Magn. Magn. Mater.* **2003**, *261*, 21.
[13] W. Lou, S. R. Nagel, T. F. Rosenbaum, R. E. Rosenweig, *Phys. Rev. Lett.* **1991**, *67*, 2721.
[14] R. Sappey, E. Vincent, N. Hadacek, F. Chaput, J. P. Boilot, D. Zins, *Phys. Rev. B* **1997**, *56*, 14551.
[15] M. Hanson, C. Johnson, S. Marup, *J. Phys. Condens. Matter* **1995**, *7*, 9263.
[16] S. Linderoth, L. Balcelles, A. Labarta, J. Tejada, P. V. Hendriksen, S. A. Sethi, *J. Magn. Magn. Mater.* **1993**, *124*, 269.
[17] S. Gider, D. D. Awschalom, T. Douglas, K. Wong, S. Mann, J. Cian, *J. Appl. Phys.* **1996**, *79*, 5324.
[18] J. Tejada, X. X. Zhang, E. Del Barco, J. M. Hernandez, E. M. Chudnovsky, *Phys. Rev. Lett.* **1997**, *79*, 1754.
[19] J. R. Freidman, U. Voskoboynik, M. P. Sarachic, *Phys. Rev. B* **1997**, *56*, 10793.
[20] S. H. Sun, C. B. Murray, D. Weller, L. Folks, A. Moser, *Science* **2000**, *287*, 1989.
[21] H. W. Gu, R. K. Zheng, X. X. Zheng, B. Xu, *J. Am. Chem. Soc.* **2004**, *126*, 5664.
[22] H. Kachkachi, W. T. Coffey, D. S. Crothers, A. Ezzir, E. C. Kennedy, M. Nogues, E. Tronc, *J. Phys. Condens. Matter* **2000**, *12*, 3077.
[23] P. P. Phule, J. M. Ginder, *MRS Bull.* **1998**, *23*, 19.
[24] J. M. Gender, *MRS Bull.* **1998**, *23*, 26.
[25] C. H. Alexiou, R. Schmid, R. Jurgons, C. H. Bergemann, F. G. Parak, W. Arnold, *J. Nanosci. Nanotechnol.* **2006**, *6*, 2762.
[26] L. Shen, A. Stachowiak, *Langmuir* **2001**, *17*, 288.
[27] S. Neveu, A. Bee, M. Robineau, D. Talbot, *J. Colloid Interface Sci.* **2002**, *255*, 293.
[28] M. T. Eloia, E. Azevedob, E. Limac, A. Pimentac, P. C. Morais, *J. Magn. Magn. Mater.* **2005**, *289*, 168.
[29] L. Shen, P. E. Laibinis, T. A. Hatton. *Langmuir* **1999**, *15*, 447.
[30] Q. Li, Y. M. Xuan, J. Wang, *Exp. Therm. Fluid Sci.* **2005**, *30*, 109.
[31] G. D. Mendenhall, Y. P. Geng, J. H. Wang, *J. Colloid Interface Sci.* **1996**, *184*, 519.
[32] M. Kroell, M. Pridoehl, G. Zimmermann, L. Pop, S. Odenbach, A. Hartwig, *J. Magn. Magn. Mater.* **2005**, *289*, 21.
[33] W. H. Butler, X. G. Zhang, D. M. C. Nicholson, T. C. Schulthess, J. M. MacLaren, *Phys. Rev. Lett.* **1996**, *76*, 3216.
[34] H. Q. Cao, Z. Xu, H. Sang, D. Sheng, T. Y. Tie, *Adv. Mater.* **2001**, *13*, 121.
[35] D. V. Goia, E. Matijevic, *New J. Chem.* **1998**, *22*, 1203.
[36] F. Fievet, J. P. Lagier, M. Figlarz, *MRS Bull.* **1989**, 29.
[37] M. Figlarz, C. Ducamp-Sanguesa, F. Fievet, J. P. Lagier, *Adv. Powder Metall.* **1992**, *1*, 179.
[38] R. E. Dunin-Borkowski, M. R. McCartney, R. B. Frankel, D. A. Bazylinski, M. Posfai, P. R. Busic, *Science* **1998**, *282*, 1868.
[39] P. Fulmer, M. Manivel Raja, A. Manthiram, *Chem. Mater.* **2001**, *13*, 2160.
[40] S. Bodea, L. Vignon, R. Ballou, P. Molho, *Phys. Rev. Lett.* **1999**, *83*, 2612.
[41] E. M. Furst, C. Suzuki, M. Fermigier, A. P. Gast, *Langmuir* **1998**, *14*, 7334.
[42] H. Niu, Q. Chen, M. Ning, Y. Jia, X. Wang, *J. Phys. Chem. B* **2004**, *108*, 3996.
[43] R. Sheparovych, Y. Sahoo, M. Motornov, S. Wang, H. Luo, P. N. Prasad, I. Sokolov, S. Minko, *Chem. Mater.* **2006**, *18*, 591.
[44] A. K. Vuppu, A. A. Garcia, M. A. Hayes, *Langmuir* **2003**, *19*, 8646.
[45] S. Sun, *Adv. Mater.* **2006**, *18*, 393.
[46] J. C. Love, A. R. Urbach, M. G. Prentiss, G. M. Whitesides, *J. Am. Chem. Soc.* **2003**, *125*, 12696.
[47] B. A. Grzybowski, H. Stone, G. Whitesides, *Nature* **2000**, *405*,1033.
[48] Z. Y. Tang, N. Kotov, *Adv. Mater.* **2005**, *17*, 951.
[49] A. K. Boal, B. L. Frankamp, O. Uzun, M. T. Tuominen, V. M. Rotello, *Chem. Mater.* **2004**, *16*, 3252.
[50] T. Fried, G. Shemer, G. Markovich, *Adv. Mater.* **2001**, *13*, 1158.
[51] J. Gao, B. Zhang, X. Zhang, B. Xu, *Angew. Chem.* **2006**, *118*, 1242; *Angew. Chem. Int. Ed.* **2006**, *45*, 1220.
[52] D. N. Srivastava, N. Perkas, A. Zaban, A. Gedanken, *Pure Appl. Chem.* **2002**, *74*, 1509.
[53] Z. Li, C. Han, *J. Mater. Sci.* **2006**, *41*, 3473.
[54] J. P. Chen, C. M. Sorensen, K. J. Klabunde, G. C. Hadjipanayis, *Phys. Rev. B* **1995**, 11527.
[55] R. Rene Van, *J. Phys. Condens. Matter* **2000**, *12*, A263.
[56] M. D. Haw, *J. Phys. Condens. Matter* **2002**, *14*, 7769.

Received: July 20, 2008
Published online: September 24, 2008

  